Small core optical waveguides are more nonlinear than expected: experimental confirmation

Shahraam Afshar V.,* Wen Qi Zhang, Heike Ebendorff-Heidepriem, and Tanya M. Monro

Institute for Photonics and Advanced Sensing, School of Chemistry & Physics, University of Adelaide, Adelaide, South Australia 5005, Australia

Corresponding author: shahraam.afshar@adelaide.edu.au

Received July 31, 2009; revised September 30, 2009; accepted October 12, 2009; posted October 23, 2009 (Doc. ID 115138); published November 12, 2009

For the first time, to our knowledge, we demonstrate the experimental confirmation of a new vectorially based expression of the effective nonlinear coefficient γ in bismuth suspended core fibers with core diameters of around 500 nm. The new expression predicts a significantly higher value of γ than what is expected based on the standard expression. We confirm that there is a distinguishable difference between the standard and our new vectorially based γ's, owing to the high index glass and subwavelength dimension of this fiber, and we show that the experimental result of γ matches the new expression within the experimental error. © 2009 Optical Society of America

OCIS codes: 190.4360, 190.4370, 190.3270, 130.4310, 060.4005, 060.5530.

Recently there has been significant interest in the design and manufacturing of waveguides with high refractive index materials and subwavelength structures (HIS-WGs) [1,2]. Such waveguides can be designed to exhibit maximal light confinement, and hence enhanced nonlinearity, which makes them attractive for a variety of nonlinear devices and applications [1–3]. Despite the enormous interest, the theory that describes nonlinear pulse propagation in these waveguides (referred to here as the standard theory), the nonlinear Schrödinger equation (NSE), still mainly relies on the well-known scalar Helmholtz equation [4]. This equation is based on the weak guidance approximation, which breaks down in HIS-WGs [3]. For a full review of recent attempts by different research groups to generalize the NSE, see [3,5] and references therein.

We have recently reported [3,5] the development of a vectorially based nonlinear Schrödinger equation (VNSE) with new vectorially based expressions of the effective nonlinear coefficient γ and Raman gain g_R for HIS-WGs. Based on these expressions, we predicted significantly higher values of γ and g_R in the HIS-WG parameter regime compared with those expected from the standard theory. We attributed these results to the large z (along the direction of the propagation) component of the propagating modes.

The main goal of this Letter is to provide a conclusive experimental confirmation of higher γ values of HIS-WGs (compared with those expected from the standard theory), which was predicted by the VNSE [3]. To the best of our knowledge, (a) this is the first time the Kerr nonlinearity of HIS-WGs has been explicitly tested for a range of subwavelength dimensions, and (b) this is the first time one aspect of the new VNSE theory, unexpectedly higher Kerr nonlinearity, is tested and confirmed experimentally. The standard effective Kerr nonlinear coefficient of a fiber, used to date, is expressed as [4]

$$\gamma^S = (2\pi/\lambda) n_2 / A_{\text{eff}}^S, \tag{1}$$

where the label S indicates standard. In our VNSE model, the effective nonlinear coefficient of a single mode highly birefringent waveguide (considering only one polarization) is modified and given by [3]

$$\gamma^V = \frac{2\pi}{\lambda} \frac{\overline{n_2}}{A_{\text{eff}}^V}, \tag{2}$$

where $\bar{n}_2$ and A_{eff}^V are given as

$$\overline{n_2} = \left(\frac{\varepsilon_0}{\mu_0}\right) k_0 \frac{\int n^2(x,y) n_2(x,y) [2|\mathbf{e}|^4 + |\mathbf{e}^2|^2] \mathrm{d}A}{3\int |(\mathbf{e}\times\mathbf{h})\cdot\hat{z}|^2 \mathrm{d}A}, \tag{3}$$

$$A_{\text{eff}}^V = \frac{\left|\int (\mathbf{e}\times\mathbf{h})\cdot\hat{z}\,\mathrm{d}A\right|^2}{\int |(\mathbf{e}\times\mathbf{h})\cdot\hat{z}|^2 \mathrm{d}A}. \tag{4}$$

Here, $\mathbf{e}$ and $\mathbf{h}$ are the electric and magnetic vector fields of the propagating mode and $n(x,y)$ and $n_2(x,y)$ are the linear and nonlinear refractive index distributions, respectively. Equation (2) has a similar form to Eq. (1) except that here $\overline{n_2}$ is the nonlinear refractive index averaged over an inhomogeneous cross section weighted with respect to field distributions, and also A_{eff}^V is given by Eq. (4) instead of the standard expression $A_{\text{eff}}^S = |\int |\mathbf{e}_t|^2 \mathrm{d}A|^2 / \int |\mathbf{e}_t|^4 \mathrm{d}A$, where $\mathbf{e}_t$ is the transverse electric field.

Equations (2)–(4) predict [3] a significant difference between the standard γ^S and the new vectorially based γ^V even for simple step-index rod waveguides, especially with high index materials, in the regime of subwavelength dimensions (nanowires). For silica nanowires γ^V can be as large as $1.3\gamma^S$, whereas for bismuth and silicon nanowires the difference can reach a factor of 2 ($\gamma^V \approx 2\gamma^S$) [3]. The important feature of the comparison between γ^S and γ^V of a nanowire is that, unsurprisingly, the two values approach each other for large core diameters, i.e., $D \gtrsim \lambda$, but differ significantly for $D \ll \lambda$, around the peak of γ versus D curve (Fig. 1).

Here, we present thorough experimental results that confirm the validity of the new vectorially based expression of γ, i.e., γ^V in the operating regime of HIS-WGs. The preliminary results of this study reporting much higher γ values than what is expected based on γ^S in a fiber with a subwavelength core size (fiber C here with a diameter of $D=530$ nm) have been reported in [6]. Here, however, we report the results of three new fabricated fibers A, B, and D (core sizes of 440, 507, and 555 nm, respectively) and their extensive and detailed measurements of loss and γ.

We first compare previously reported experimental values for the highest γ in different waveguides with the calculated values of γ based on the standard and vectorial expressions, i.e., γ^S and γ^V, respectively. Figures 1(a)–1(c) show the recorded experimental values of γ for a few bismuth [7] and SF57 [8,9] suspended core microstructured optical fibers (MOFs) and chalcogenide nanowires [10,11], respectively, together with the numerical modeling results of γ^S and γ^V. For the suspended core MOFs, the original scanning electron microscope (SEM) image of one of the fibers [insets in Figs. 1(a) and 1(b)] is scaled to reduce or increase the core diameter. For each diameter, we have used a finite-element package, COMSOL 3.4, to calculate the mode field distributions from which we have calculated γ^S and γ^V values. For the chalcogenide tapered fibers (nanowire) [10,11], we have used the analytical solutions of the Maxwell's equations to find the mode field distributions and calculate γ^S and γ^V. Comparing the measured γ values for different bismuth ($n=2.02$ and $n_2=3.2 \times 10^{-19}$ m^2/W) [7], SF57 ($n=1.81$ and $n_2=4.1 \times 10^{-19}$ m^2/W) [8], and chalcogenide ($n=2.8$ and $n_2 = 1.1\times 10^{-17}$ m^2/W [10]) fibers in Figs. 1(a)–1(c), respectively, with the theoretical calculations according to γ^S and γ^V expressions indicates that for the corresponding core diameters there are no distinguishable differences between the two theoretical models. Recently, we have been able to fabricate suspended core fibers with core diameters in the range of $D \approx 400-700$ nm [12]. Using this new method, we have been successful to fabricate a suspended core bismuth fiber with a core diameter of only 530 nm [13]. Further refinement of the fabrication technique has recently led to similar fibers with the core diameter of $D=555$ nm and even smaller diameters of $D=507$ and 440 nm.

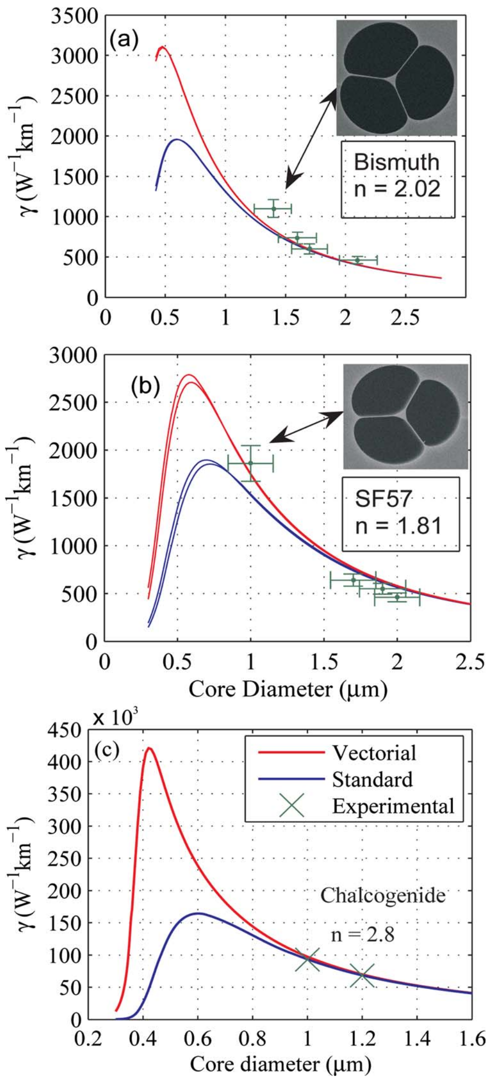

Fig. 1. (Color online) (a) Previously reported experimental values (data points) [7–9] and numerical results of γ^V and γ^S versus core diameter for (a) bismuth, (b) SF57 suspended core, and (c) chalcogenide [10,11] tapered (nanowire) fibers.

For each fiber, we have measured the effective nonlinear coefficient γ using the dual-cw method [6,14]. These fibers are effectively single mode at $\lambda \approx 1550$ nm, and we have bent the fibers and covered them with Dag graphite fluid to effectively remove the cladding and high-order modes. Loss measurement was the main source of uncertainty (through the effective length) in extracting the γ values, from the nonlinear phase shifts. Owing to the high loss of these fibers (compared with the typical loss of our micrometer-scale core fibers of ~1 dB/m, when made from the same bismuth glass) the effective lengths of these fibers were limited, and the uncertainty in γ increased rapidly as a function of L. Thus, we measured the nonlinear phase shift for fiber lengths close to maximum effective lengths of each fiber (21, 36, 31, and 54 cm for fibers A, B, C, and D, respectively). For the loss measurements, we cut several 1-m-long pieces of each fiber and performed nine to ten cutback measurements for every 1 m section to evaluate the average attenuation of each individual 1 m section. We also estimated the statistical variation of the average attenuation of 1 m sections along the fiber (Fig. 2 and the inset). The overall uncertainty in the loss measurement is due to both uncertainties in the measurements of the core mode power and fiber length and the statistical fluctuation of the attenuation along the fiber. While the statistical fluctuations of attenuation values for fibers B, C, and D were similar to those owing to power and length measurements, they were significantly higher for fiber A—with the smallest core diameter (see Fig. 2 and

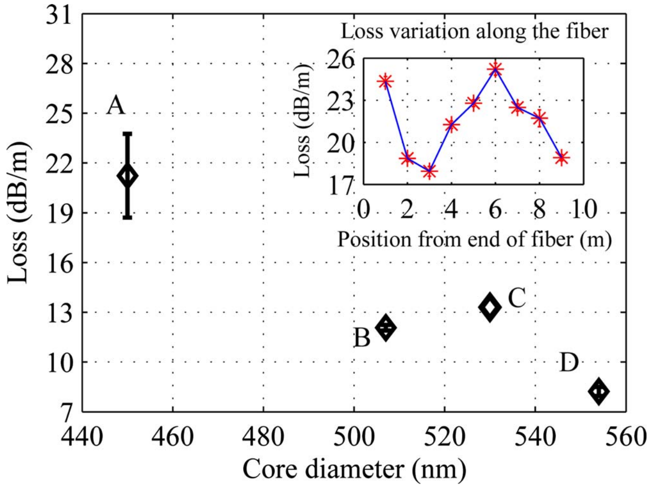

Fig. 2. (Color online) Loss measurements values for four fibers A, B, C, and D. Average attenuation of successive 1 m pieces of fiber A is shown in the inset. Every point in the inset is the average of nine or ten cutback loss measurements.

the inset)—and represent the main source of uncertainty. The source of this high statistical uncertainty could be related to fluctuations during the fiber drawing process, including fluctuations in the fiber outer diameter ($\pm 2\ \mu$m) or glass temperature. The attenuation versus core diameter result, as shown in Fig. 2, is consistent with the fact that the loss of optical nanowires (either suspended or free standing) increases rapidly as D decreases [12]. This is attributed to the increase in the field strength at the hole interfaces, which leads to a larger roughness scattering loss component.

The glass used in the fiber is bismuth borosilicate, which is different from the one reported in [7] (bismuth silicate) and is provided by Asahi Glass Co. It has a lower refractive index of $n=1.9771$ at 1550 nm but a higher nonlinear refractive index of $n_2=6.0 \times 10^{-19}\ \mathrm{m}^2/\mathrm{W} \pm 10\%$ at 1550 nm [6]. We have calculated the field distributions of the real fiber by using the SEM image of fiber C shown in the inset of Fig. 3

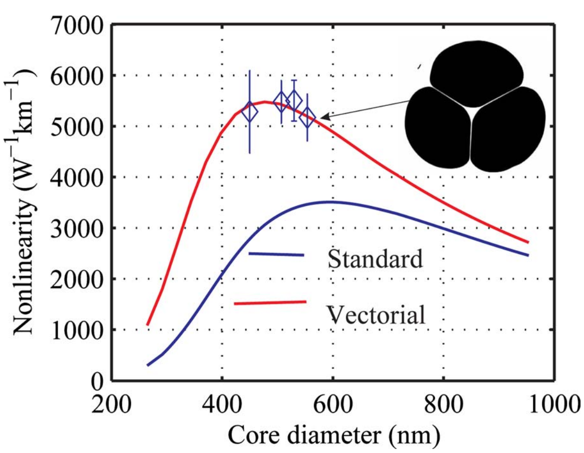

Fig. 3. (Color online) Experimental values (data points) and calculated curves of γ [according to standard (bottom curve) and vectorial (top curve) expressions] for fibers as in Fig. 2.

and a finite-element method. By scaling up (down) of the structure, we have got different core diameter suspended core fibers, which have been used to calculate γ^S, γ^V for different core diameters. Figure 3 then shows the plots of γ^S and γ^V as functions of the core diameter, achieved by scaling the fiber. The experimental results of γ are also shown for the four fibers. An excellent agreement between the experimental results and the vectorially based expression of γ, γ^V is observed, confirming the validity of this expression in the HIS-WG regime. This confirms one of the predictions of the new VNSE model, namely, the Kerr nonlinearity enhancement in HIS-WGs [3]. It is expected that the new expression of γ, i.e., γ^V, and new VNSE model significantly impact the design and performance of nonlinear HIS-WGs.

We acknowledge Asahi Glass Co. Japan for the supply of the bismuth glass. This research was supported under the Australian Research Council (ARC) Linkage funding scheme. T. M. Monro acknowledges the support of an ARC Federation Fellowship.

References

1. M. Pelusi, F. Luan, T. D. Vo, M. R. E. Lamont, S. J. Madden, D. A. Bulla, D.-Y. Choi, B. Luther-Davis, and B. J. Eggleton, Nature Photon. **3**, 139 (2009).
2. C. Koos, P. Vorreau, T. Vallaitis, P. Dumon, W. Bogaerts, R. Baets, B. Esembeson, I. Biaggio, T. Michinobu, F. Diederich, W. Freude, and J. Leuthold, Nature Photon. **3**, 216 (2009).
3. S. Afshar V. and T. M. Monro, Opt. Express **17**, 2298 (2009).
4. P. Agrawal, *Nonlinear Fiber Optics* (Academic, 2007).
5. M. D. Turner, T. M. Monro, and S. Afshar V., Opt. Express **17**, 11565 (2009).
6. S. Afshar V., W. Zhang, and T. M. Monro, in *CLEO/IQEC 2009 Proceedings* (Optical Society of America, 2009), paper CThBB6.
7. H. Ebendorff-Heidepriem, P. Petropoulos, S. Asimakis, V. Finazzi, R. Moore, K. Frampton, F. Koizumi, D. Richardson, and T. Monro, Opt. Express **12**, 5082 (2004).
8. H. Ebendorff-Heidepriem, P. Petropoulos, V. Finazzi, S. Asimakis, J. Leong, F. Koizumi, K. Frampton, R. C. Moore, D. J. Richardson, and T. M. Monro, in *OFC 2005 Proceedings* (Optical Society of America, 2005), paper OThA3.
9. J. Y. Y. Leong, P. Petropoulos, J. H. V. Price, H. Ebendorff-Heidepriem, S. Asimakis, R. C. Moore, K. E. Frampton, V. Finazzi, X. Feng, T. M. Monro, and D. J. Richardson, J. Lightwave Technol. **24**, 183 (2006).
10. E. C. Magi, L. B. Fu, H. C. Nguyen, M. R. E. Lamont, D. I. Yeom, and B. J. Eggleton, Opt. Express **15**, 10324 (2007).
11. D.-I. Yeom, E. C. Mägi, M. R. Lamont, M. A. Roelens, L. Fu, and B. J. Eggleton, Opt. Lett. **33**, 660 (2008).
12. H. Ebendorff-Heidepriem, S. C. Warren-Smith, and T. M. Monro, Opt. Express **17**, 2646 (2009).
13. W. Q. Zhang, S. Afshar V., H. Ebendorff-Heidepriem, and T. M. Monro, Electron. Lett. **44**, 1453 (2008).
14. A. Boskovic, S. V. Chernikov, J. R. Taylor, L. G. Nielsen, and O. A. Levring, Opt. Lett. **21**, 1966 (1996).